FLUENT ANALYSIS OF A ROSA COLD LEG STRATIFICATION TEST

T. Farkas, I. Tóth

Hungarian Academy of Sciences KFKI Atomic Energy Research Institute
Budapest P .O. Box 49, 1525 Hungary

Abstract

One of the OECD ROSA project tests, investigating temperature stratification in the cold legs and the downcomer during ECCS water injection under single-phase natural circulation conditions was analysed with the FLUENT code. The guidance given in the „Best Practice Guidelines for the Use of CFD in Nuclear Reactor Safety Applications" of the OECD GAMA group was followed. Steady-state calculations were performed with the Standard k-ε, the Realizable k-ε and the Reynolds Stress Model, the last one being closest to the measured results. The calculations indicate the predominance of buoyancy effects in the cold leg caused by the density difference between cold and hot water, while in the test it seems, as if mixing between the cold plume and hot water would be the prevailing mechanism. It is shown that the temperature distribution in the downcomer is strongly influenced by correct modelling of the cold leg-downcomer connection. A model with an abrupt transition leads to the colder fluid flowing to the core barrel, while in the test it was flowing down along the vessel wall. Approximating the rounded transition with a radius of 19 mm in the ROSA facility by a 45^o expansion zone led to a shift of the cold stream towards the vessel wall.

1. INTRODUCTION

Pressurised Thermal Shock (PTS) still remains an issue in nuclear reactor safety. Severe PTS transients are featured by cold Emergency Core Cooling (ECC) water injection into stagnating coolant in the primary circuit. In such a case the resulting flow pattern is governed primarily by buoyancy forces, i.e. thermal stratification and mixing of the cold and hot water play a dominant role. Due to the important 3D effects, these phenomena cannot be predicted with thermal hydraulic systems codes: a realistic description of the mixing process can only be expected from CFD codes. In a recent OECD survey (Smith, 2008) PTS is listed among the relevant safety issues and available test data as well as recent analyses are reviewed.

Within the EU FLOMIX-R project the computer codes FLUENT and ANSYS-CFX were validated against Tests 10, 20, and 21 of the IVO test facility, modelling a VVER-440 downcomer (Rohde, 2004). The Test 20 was analysed by the FLUENT code (Toppila, 2002). The model included the cold legs with safety injection line and he used 283000 cells. The thermal stratification in the cold leg and reactor downcomer was examined, and the asymmetrical stratification under the cold leg corresponds to the experimental results.

Important PTS data base has been created in the Upper Plenum Test Facility (UPTF), although the data are proprietary. UPTF is a 1:1 model of a 1300 MWe Siemens/KWU PWR. The UPTF Test 1 was simulated by the ANSYS CFX code using different Reynolds Averaged Navier Stokes (RANS) models (Willemsen, 2005). In this test, the primary system was initially filled with stagnant hot water at 190°C. The cold ECC water, at 27°C, was injected into one cold leg with a mass flow rate of 40 kg/s. The authors found that the location of the cold plume along the downcomer thickness depended on modelling of buoyancy as well as on correct modelling geometrical details, like reactor lower plenum internals. For example, inclusion of detailed models of internals, which should improve the results since they are closer to reality, reduced circumferential temperature oscillations in the downcomer. As a result, the cold ECC water was flowing primarily along the core barrel, whereas an alternating hot and cold fluid was seen to pass the core barrel and vessel wall in the experiment. Therefore, the cooling of the RPV wall is significantly underestimated in the computation.

In the OECD ROSA project, new tests with more detailed instrumentation have been carried out to investigate stratification in the cold legs and temperature distribution in the downcomer during ECCS water injection under single- and two-phase natural circulation conditions in the primary system. The main aim of the tests is to supply additional, high quality data for validation of CFD tools.

One of these tests, T1-1 has been analysed using the FLUENT code. Throughout the analysis, special consideration was given to the Best Practice Guidelines (BPG) for the use of CFD in nuclear safety applications developed in the framework of the OECD CSNI (Mahaffy et al., 2007). The calculations presented are the first post-test results for the ROSA T1-1 experiment. Since OECD project results are proprietary for a given period of time after termination of the project, test results can only be reported here in a qualitative way.

2. THE ROSA STRATIFICATION TEST

One of the test series performed within the OECD ROSA project investigates temperature stratification in the cold legs and the downcomer during ECCS water injection under single- and two-phase natural circulation conditions. The first test, T1-1 addressed the issue in quasi steady-state conditions at different mass inventories. The initial condition of the test corresponded to single-phase natural circulation at 15.5 MPa at 100 % primary inventory with a core power corresponding to 2 % of the scaled nominal power. ECCS water with a temperature of 300 K is injected into the cold legs A and B one after another during a period of 80 s, applying two different ECC flow rates. The injections were initiated at about 10 minute intervals in order to allow re-stabilization of the system.

Multidimensional temperature distributions were measured by rakes of thermocouples. In the cold legs, these were located in three cross-sectional planes, as shown in Fig. 1: one below the injection point (containing 9 thermocouples) and two more between injection and downcomer, each containing 21 thermocouples, as shown by Fig. 2. 18 thermocouples were installed in the downcomer below each cold leg (Fig. 3).

The nominal accuracy of the thermocouple measurements is +/- 2.75 K. However, calibration performed with uniform temperature in the cold legs prior to starting the test allowed to reduce this value even further.

For the analysis with the FLUENT code, the first injection to cold leg A in T1-1 was selected, when the primary system inventory corresponded to the nominal one. The cold leg A was chosen, since there the ECC injection is perpendicular to the main stream, as it is the case in VVER-type reactors. From the two injections at 100 % primary inventory the one with lower flow rate was chosen, since it was closer to typical VVER conditions.

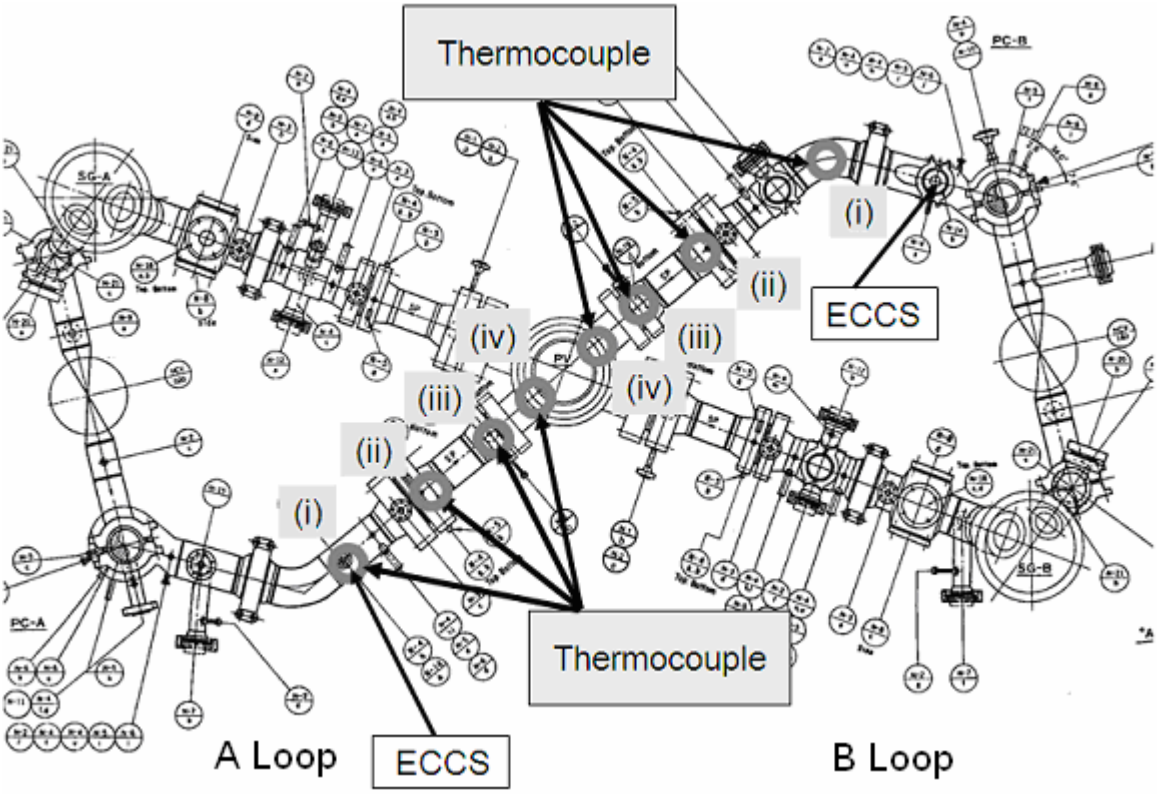

Fig. 1: Locations of new thermocouples in cold legs and downcomer

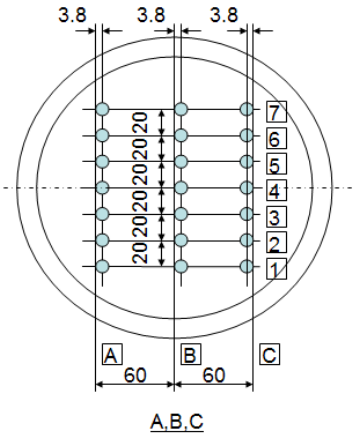

Fig. 2: Locations of thermocouples in cold leg A, at sections ii and iii of Fig. 1

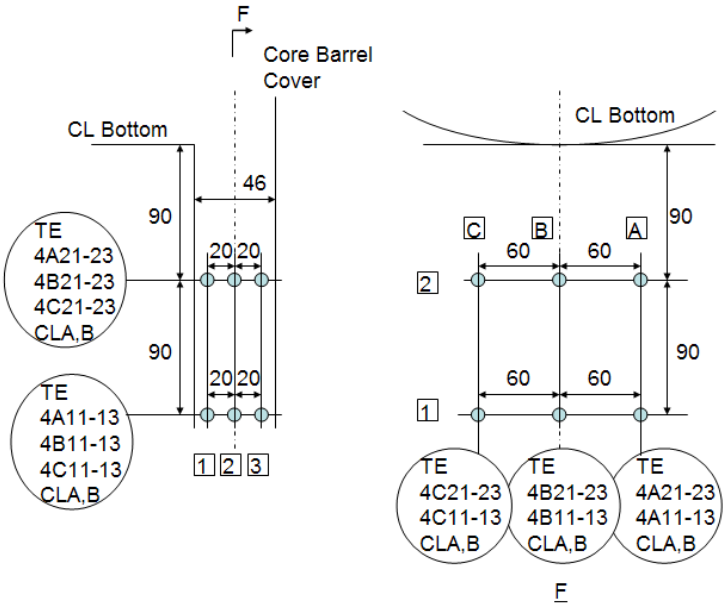

Fig. 3: Locations of new thermocouples in the downcomer

3. FLUENT ANALYSIS

The analysis was performed by the version 6.3.26 of FLUENT with the aim to validate the code for PTS-type calculations, when the phenomena are strongly influenced by buoyancy effects. Due to the large temperature difference between cold leg and ECCS injection, the fluid densities differed by about 20 %. At each step of the analysis, e.g. grid generation, selection of turbulence model, discretization scheme etc., special effort was done to follow the Best Practice Guidelines (BPG) for

the use of CFD in nuclear safety applications developed in the framework of the OECD CSNI (Mahaffy et al., 2007).

For the FLUENT calculation only the cold leg of loop A was modelled downstream of the pump, including the bend upstream of the ECCS injection, as shown by Fig. 4. Half of the downcomer was modelled, its height being limited to 1340 mm. Mass flow rates were given at the pump in the cold leg and in the ECCS line, while a pressure boundary was imposed at the lower part of the downcomer. The non-modelled half of the downcomer was taken into account by symmetry boundary conditions.

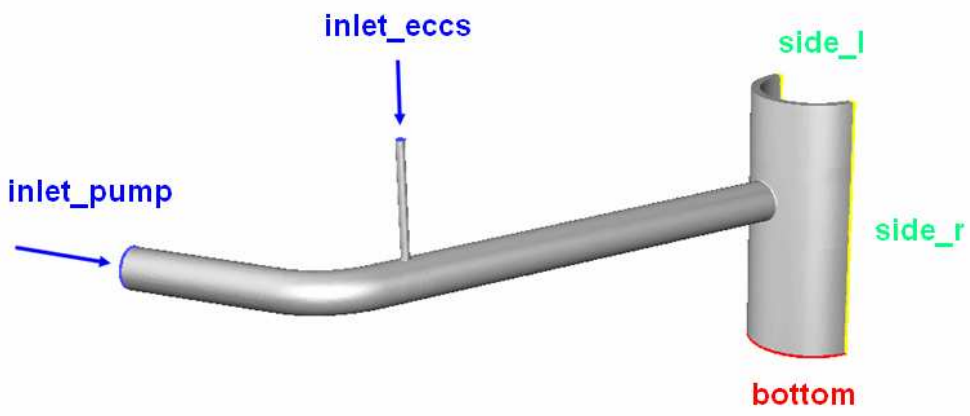

Fig. 4: FLUENT model with boundary conditions

3.1 Grid Generation

As proposed by the BPG a structured mesh consisting of 668288 hexahedral elements was developed with special care for meshing around ECC line/cold leg and cold leg/downcomer connection. The guidelines for cell skewness, cell size change between adjacent cells and cell aspect ratio were taken into account and the corresponding requirements fulfilled.

Mesh parameters	From value	To value
Skewness	0	0.611
Size change	0.8	1.9
Aspect ratio	1	4

3.2 Boundary Conditions

The measured temperature distribution in the cross section of the cold leg, 0.7 m down-stream of the injection point is presented in Fig. 5. It can be seen that the test can be regarded as a quasi-steady-state process during the later phase of the 80 s injection, therefore it was decided to do steady-state FLUENT analysis for the period between the dashed red lines. Primary loop and ECC flow rates were practically constant in this period, and so was the loop temperature. However, the ECC water temperature was changing about 20 K in the selected period, as shown by Fig. 6, the average value between the dashed lines was applied as boundary condition. Adiabatic conditions were assumed at the walls.

The thermal properties of the water were described as polynomial functions in the range of 293 and 573 K at constant pressure, 15.5 MPa.

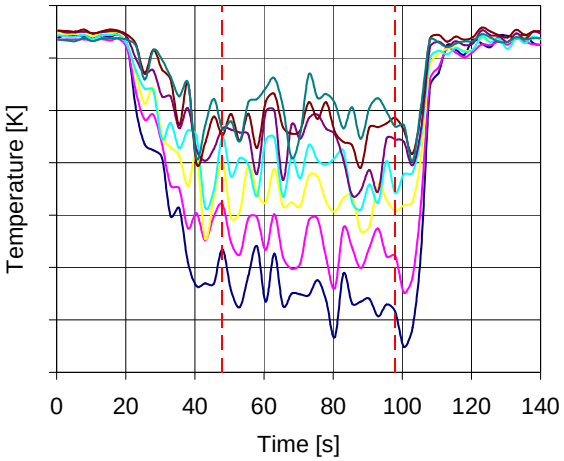

Fig. 5: Measured temperature distribution in the cross section of the cold leg, 0.7 m down-stream of the injection point

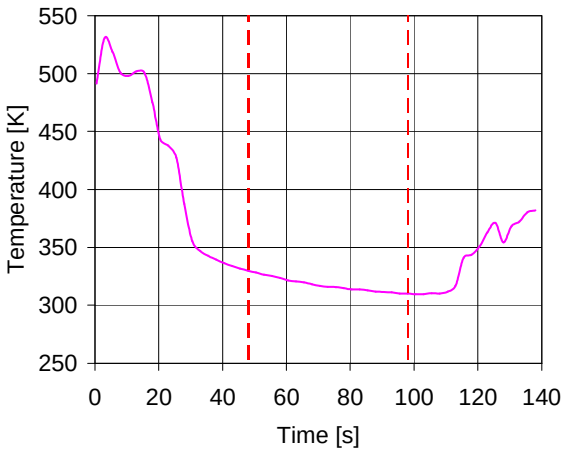

Fig. 6: Measured ECC water temperature

3.3 Calculation results

A large number of calculations have been performed, they are summarised in Table 1. FLUENT was run on a PC with an Intel Pentium4 3.2 GHz processor and a memory of 3.12 GB, under MS-WindowsXP. Typical computation time for Case 11 was about 3 days.

Table 1: The matrix of performed calculations

Case	Grid description	Grid size	Turbulence model	Discretization		Time step
				space	time	
1.	initial grid	668 288	Standard k-ε	1st	-	-
2.	initial grid	668 288	Realizable k-ε	1st	-	-
3.	initial grid	668 288	RSM	1st	-	-
4.	initial grid	668 288	Realizable k-ε	2nd	-	-
5.	ECCS line:351.5mm	665 408	Realizable k-ε	1st	-	-
6.	ECCS line:46.5mm	661 328	Realizable k-ε	1st	-	-
7.	outlet position: 1600mm down	780 288	Standard k-ε	1st	-	-
8.	ECCS line:351.5mm	665 408	Realizable k-ε	1st	1st	0.05s
9.	ECCS line:351.5mm	665 408	RSM	1st	1st	0.05s
10.	2x2x2 FLUENT refined grid	5 323 264	Realizable k-ε	1st	-	-
11.	refined grid	1 545 768	RSM	1st	-	-

Different turbulence models have been tested in the first three calculations, based on the "default" grid. Nos. 4 and 5 to 7 investigated the effect of spatial discretization and position of the boundary conditions, respectively. In order to evaluate the effect of steady-state approach, two calculations were done in the transient mode. The impact of grid refinement was also analysed. Since RSM calculations require much higher CPU time and memory, most of the parametric studies were done by the Realizable k-ε model.

In presenting the results, the focus will obviously be on the temperature distributions in the cold leg and the downcomer, since velocity distributions have not been measured. Comparison with measurements will be presented in the planes of the thermocouple rakes, as shown in Fig. 7.

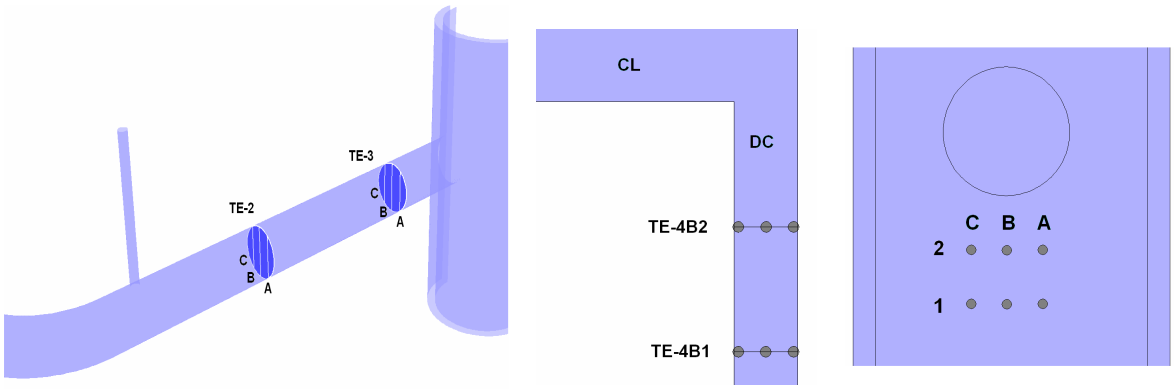

Fig. 7: Measurement planes, places of comparison

3.3.1 Turbulence Models

Three commonly used Reynolds Averaged Navier-Stokes models have been selected for the analysis: the Standard k-ε, the Realizable k-ε and the Reynolds Stress model (RSM). These models are the basic models of practically all CFD codes and – with the usually available computing capacities – the ones most widely used in the engineering practice. Since the density of the injected fluid differed by about 20 % from the main stream density, the buoyancy effects have been included in all models. The BPG proposes the RSM in case of strong buoyancy effects.

The temperature distributions in the cold leg in case of the three different turbulence models are shown in Fig. 8. In all cases temperature stratification can be observed. Surprisingly, the Standard k-ε and RSM give rather similar results: the flow is buoyancy driven. The injected cold water first hits the bottom of the cold leg and then moves almost to the top along the tube wall, indicating limited mixing with the main stream hot water. The Realizable k-ε model calculates more intensive mixing and buoyancy effects are less dominant.

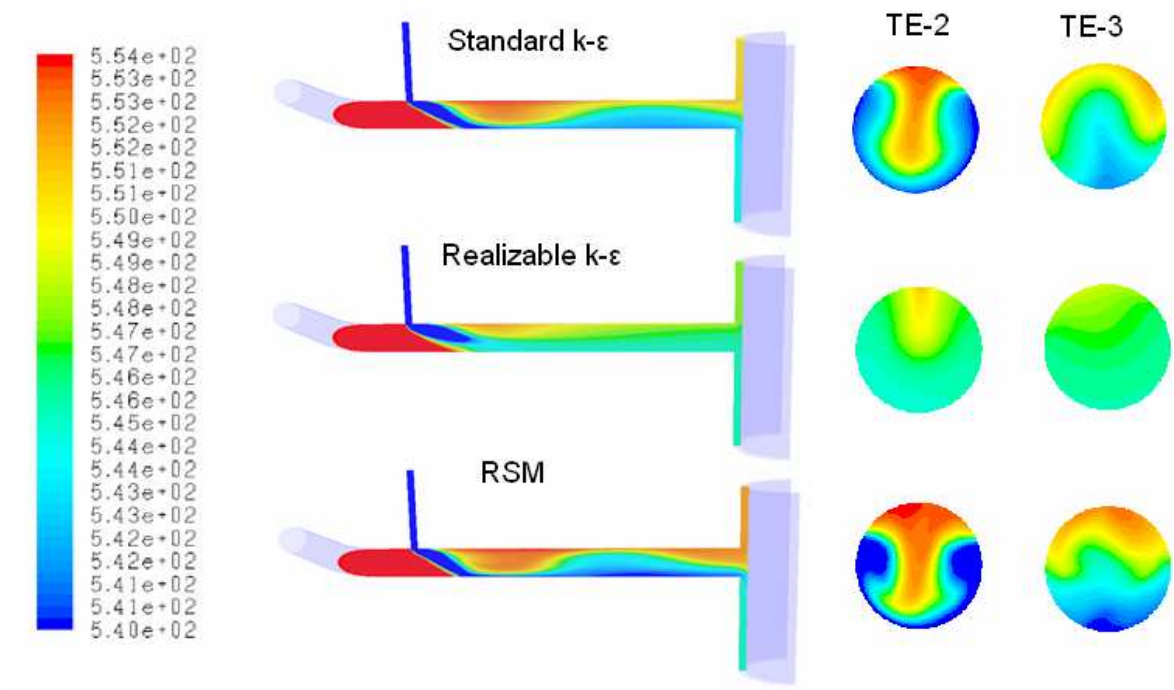

Fig. 8: Temperature distributions in the cold leg

Comparison of the measured and calculated results along the TE-2B and TE-3B lines (Fig. 9) indicates again the overestimation of the mixing with the Realizable k-ε model, especially in plane 3. It should be mentioned that the calculation does not consider the structure holding the thermocouples and the video probe (the latter installed between the injection point and plane 2), which obviously create additional turbulence.

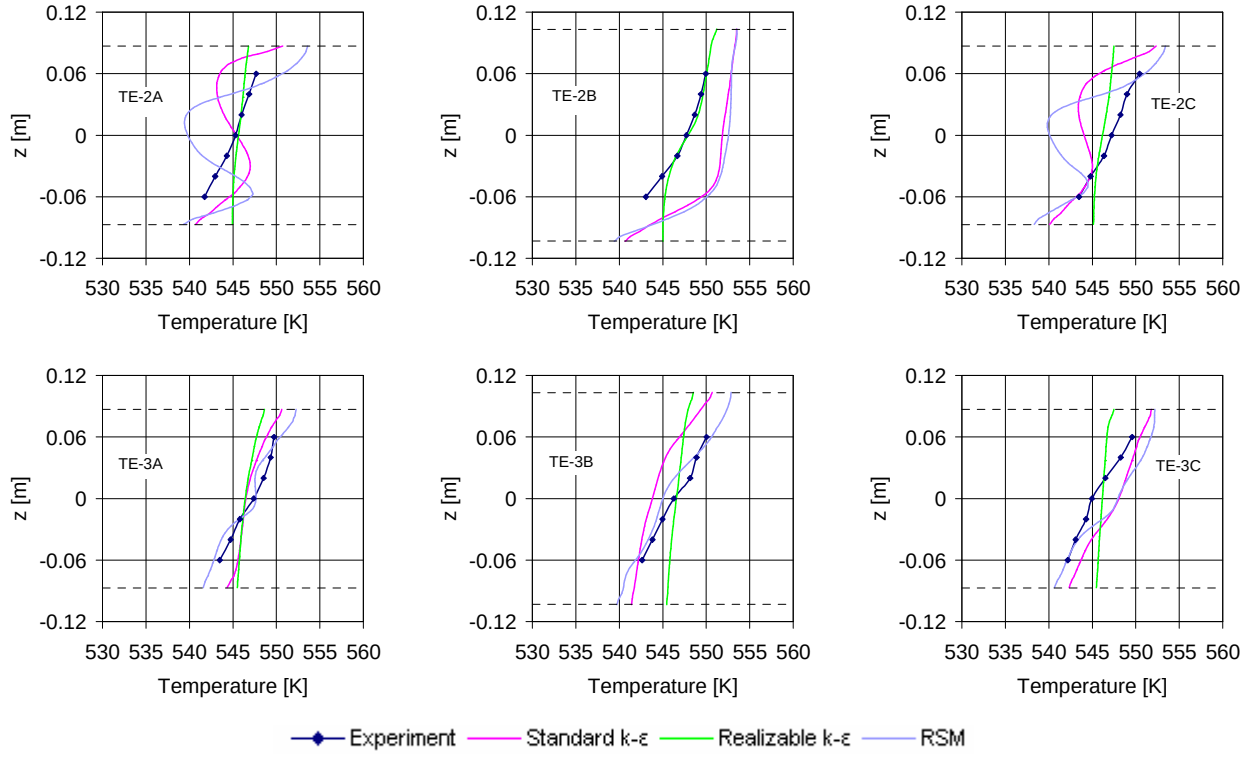

Fig. 9: Comparison of the measured and calculated results along the TE-2B and TE-3B lines

3.3.2 Discretization Scheme

Applying first or second order spatial discretization in the Realizable k-ε model produced negligible effect on the results.

3.3.3 Position of Boundary Conditions

At the selected boundaries of the modelled part of the ROSA facility, no detailed information is available concerning flow, temperature and pressure distributions and the usual approach is to assume homogeneous distributions. The BPG stresses the importance of parametric studies in such cases to demonstrate that missing distributions and/or turbulence quantities have no impact on the results.

The boundary of the cold leg inlet was defined sufficiently far away of the injection point, beyond the bend. It can be assumed that all possible non-homogeneities are "over-ridden" in the turbulent flow field until the injection point, taking into account the influence of the bend as well. This is supported both by the measurements and the calculations, which indicate only a slight cross-sectional asymmetry in plane 2 and this can be attributed to the bend.

Three different ECC line lengths have been investigated: 46.5, 351.5 and 570.5 mm, respectively. The results with the shortest injection line differ from the two other, indicating that the flow is not fully developed in the former case. The two longer tubes give identical results.

The effect of the outlet boundary was evaluated by modelling an additional 1600 mm of the downcomer: no effect on the flow structure could be found.

3.3.4 Transient Calculations

As discussed in section 3.2, the steady-state approach cannot be fully justified especially due to the change in the ECC water temperature. Therefore, two additional calculations were run with the Realizable k-ε and the RSM model, respectively in transient mode for the period 15 to 100 s in Fig. 5. In both cases, the results were very similar to the corresponding steady-state ones indicating that the primary cause of the deviations between measurement and calculation is not the considerable temperature change of the ECC water. The temperature evolution along the vertical axis of the cold leg in the planes 2 and 3 is shown in Fig. 10.

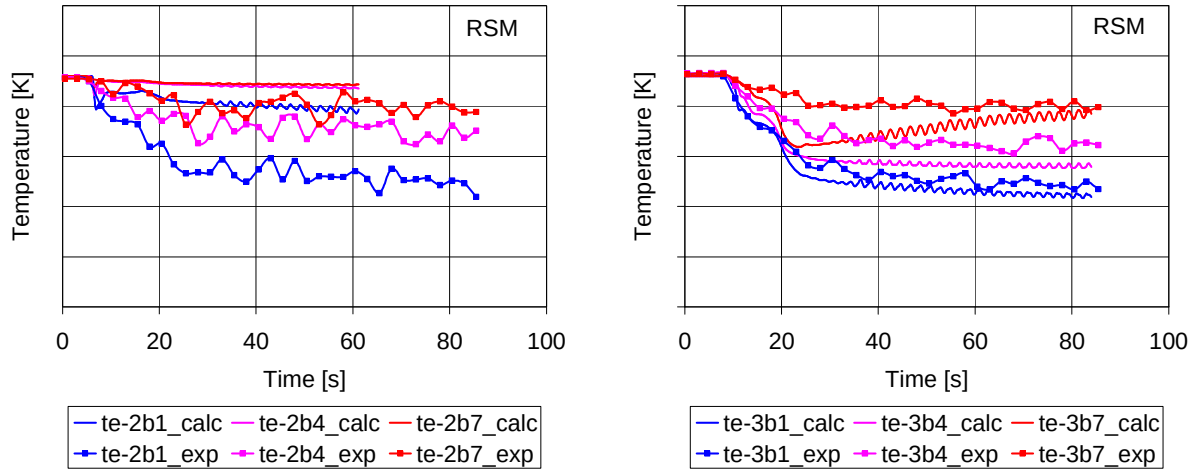

Fig. 10: Transient temperature evolution along the vertical axis of the cold leg in planes 2 and 3

3.3.5 Grid Refinement

Demonstration of grid-independence is a basic requirement in CFD analysis, however, due to insufficient computer resources, in real-life technical problems it can mostly not be achieved. A calculation was run with half of the original grid size in all directions, resulting in a model of 5 323 264 cells. As expected, this showed some difference from the results obtained with the original grid. Since it was not possible to go on with systematic grid refinement – and assuming that the carefully developed structured mesh for most of the flow-field was adequate – local refinement was performed. The resulting 1.5 million cell model applied smaller-sized cells in the injection line, in the cold leg between injection and downcomer, with special care to the near-wall region. Earlier results were especially unsatisfactory in the downcomer and it was supposed that this might be the consequence of modelling the cold leg-downcomer connection by abrupt area change. Additional information obtained from ROSA experts (Watanabe, 2008) confirmed that there is a rounded transition with a radius of 19 mm. In the new model this was represented by a 45^{o} expansion zone over a length of 19 mm.

Figure 11 compares the results with the ones presented in Fig. 8. In plane 2 there is almost no change, however, in plane 3 a higher degree of mixing can be observed with the refined model. The downcomer temperature distribution is even more affected, as shown in Fig. 12. While in the base case the cold layer at the cold leg bottom was flowing to the core barrel side, the 45^{o} transition led to a shift of the cold stream towards the vessel wall – in agreement with the measurements. The temperature distribution in plane 4 is shown in Fig. 13: it indicates good agreement left and right of the cold leg axis, while in the axis the calculated temperature next to the vessel wall is still

significantly higher than in the test. This proves the importance of correct description of the cold leg-downcomer transition.

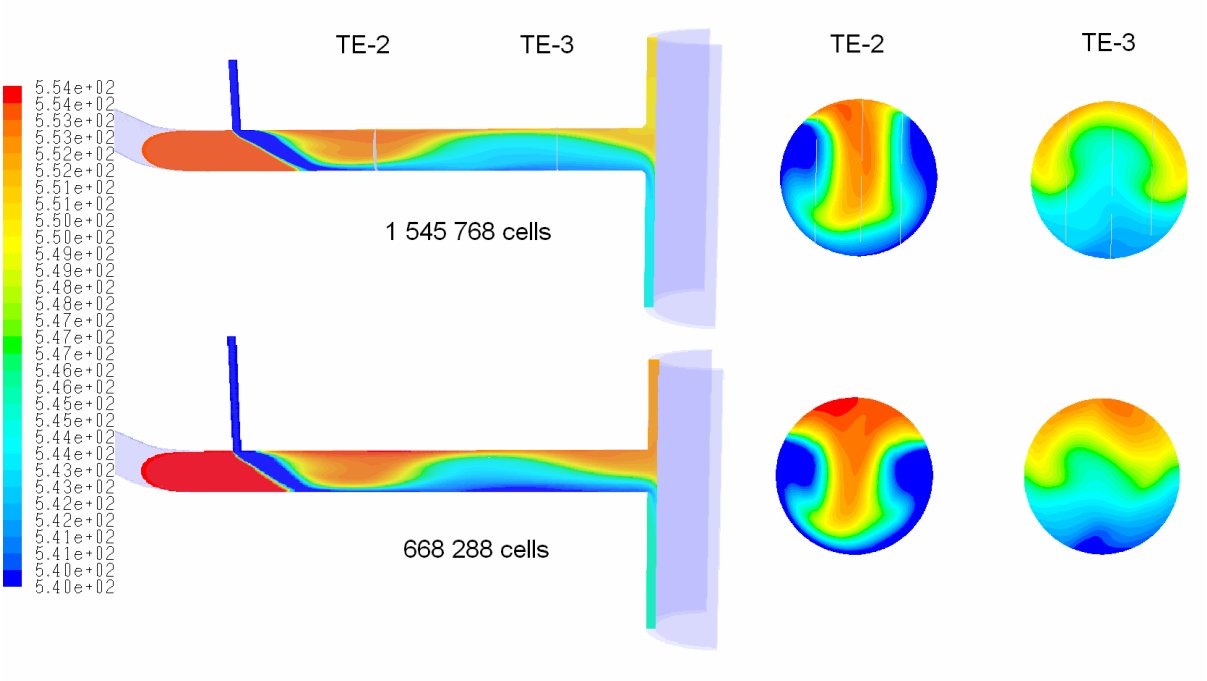

Fig. 11: Effect of local grid refinement on the temperature distribution in the cold leg

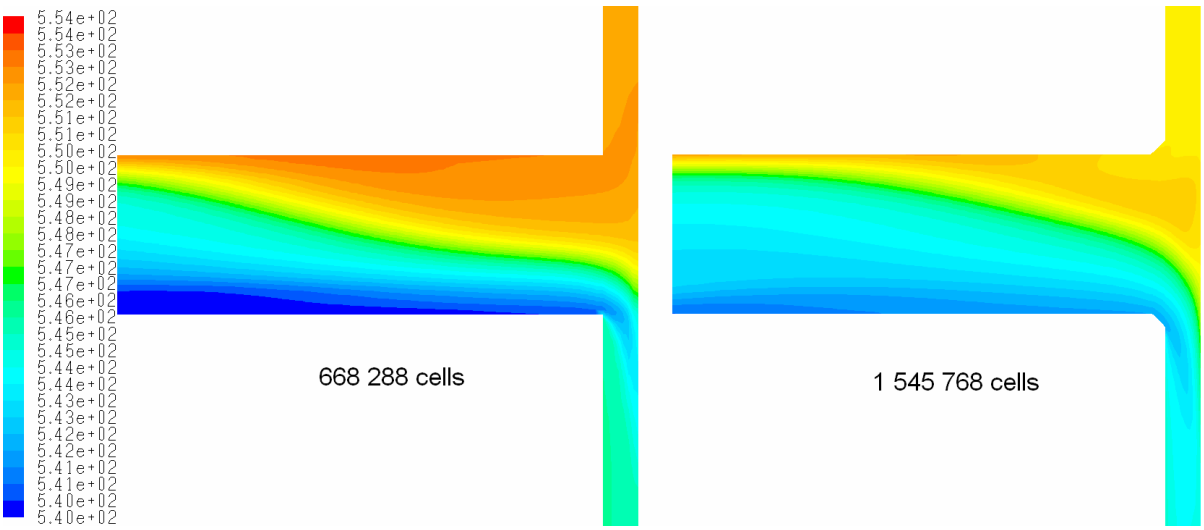

Fig. 12: Effect of local grid refinement on the temperature distribution in the downcomer

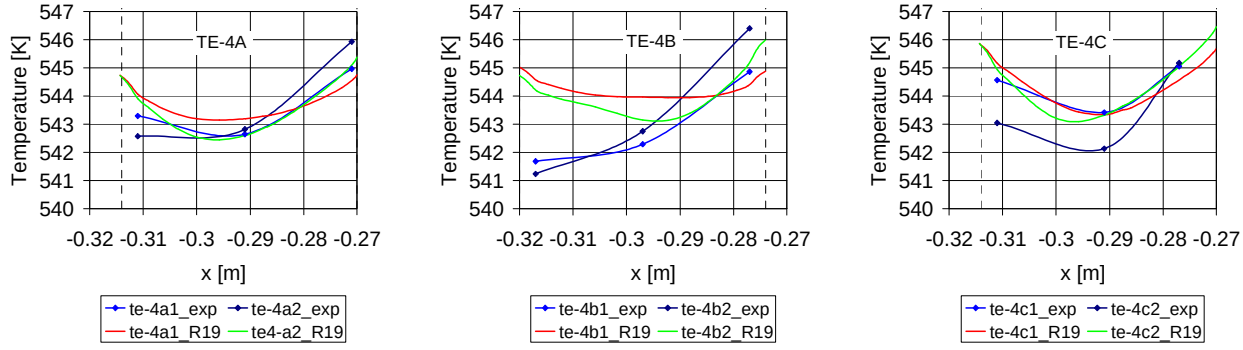

Fig. 13: Temperature distribution in the downcomer (plane 4), 1 545 768 cells

4. CONCLUSIONS

FLUENT analysis results were presented for one of the tests performed in the OECD ROSA project. The test investigates temperature stratification in the cold leg and the downcomer – initially filled with hot water – during ECCS water injection under single-phase natural circulation conditions. The calculation results were compared with multidimensional temperature distributions measured by rakes of thermocouples located in three cross-sectional planes in the cold leg and at two elevations in the downcomer.

The „Best Practice Guidelines for the Use of CFD in Nuclear Reactor Safety Applications" of the OECD GAMA group were followed both in the mesh generation process and in the analysis. A structured mesh consisting of 668288 hexahedral elements was developed with special care for meshing around ECC line/cold leg and cold leg/downcomer connection. The guidance for cell skewness, cell size change between adjacent cells and cell aspect ratio were taken into account.

A number of steady-state calculations were performed in order to check the effect of different turbulence models (Standard k-ε/ Realizable k-ε/ RSM), the spatial discretization scheme (1st/ 2nd order), grid refinement and the position of the boundary conditions.

The analysis results allow the following conclusions:

- The turbulence model applied affects the flow and temperature distribution first of all in the cold leg. It is an unexpected result that Standard k-ε and the RSM produced very similar results, both showing strong buoyancy effects and less intensive mixing of the cold plume with respect to Realizable k-ε model. In spite of these differences, the stratification process in the cold leg is captured by all models.
- Change from 1st to 2nd order discretization scheme had negligible effect on the results, which is believed to be the consequence of the thoroughly constructed grid.
- There was little difference between the results obtained with the "base grid" of 668 288 cells and the refined one (with half of the original grid size in all directions) with 5 323 264 cells. Since mesh-independence could not be demonstrated, local mesh refinement was applied in critical regions, like around the injection point, cold leg-downcomer connection and next to the wall.
- Comparison of steady-state and transient calculation results shows little difference. This indicates that the primary cause of the deviations between measurement and calculation is not the considerable temperature change of the ECC water during the analysed period.

It is difficult to draw final conclusions by comparing the measured and calculated results, since the velocity field in the cold leg can only be inferred with high uncertainty based on the measured temperature distributions. The calculations indicate the predominance of buoyancy effects caused by the density difference between cold and hot water in the cold leg: the cold ECC plume first hits the bottom of the cold leg, then, flowing on both sides of the tube reaches almost the top and, finally, tends to stratify. Based on the temperature readings of the test it seems, as if the process in ROSA would be less dominated by buoyancy than by mixing between the cold plume and hot water in the cold leg. It may be questioned to what extent this difference is caused by the mixing effect of the thermocouple rakes and the video probe installed in the flow field.

The calculated and measured temperature distribution in the downcomer show even larger divergence: while in the experiment the colder fluid at the bottom of the cold leg tends to flow down along the vessel wall, in the calculation it flows to the core barrel. It was shown that this behaviour is strongly influenced by the model of the cold leg-downcomer connection. Assuming an abrupt transition leads to what was described just above, while approximating the rounded transition with a radius of 19 mm in the ROSA facility by a 45^{o} expansion zone led to a shift of the cold stream towards the vessel wall.

It is planned to make further analysis with a more detailed resolution of the cold leg-downcomer transition.

Although the ROSA test produced high-accuracy temperature measurements, the test results offer limited possibility of CFD code validation. It is difficult to assess e.g. buoyancy effects based on the temperature distribution measured in two planes of the cold leg: this would require more detailed information about the flow field, including velocity distributions. In order to judge, whether buoyancy or turbulent mixing are the predominant factors in the observed thermal stratification, measurement of the turbulent properties would also be needed. It is planned to perform such tests using the institute's PIV/LIF technique described in another paper (Tar, 2008) that would eliminate doubts about the effect of intrusive measurements on the flow field.

5. REFERENCES

J. Mahaffy et al., "Best Practice Guidelines for the Use of CFD in Nuclear Reactor Safety Applications", NEA/CSNI/R(2007)5, (2007).

U. Rohde et al., "Validation of CFD Codes Based on Mixing Experiments. Final Report of the Work Package 4 of the FLOMIX-R Project", (2004)

B.L. Smith et al., "Assessment of CFD for Nuclear Reactor Safety Problems", NEA/CSNI/R(2007)13, (2008).

D. Tar et al., "Experimental Investigation of Coolant Mixing in VVER Reactor Fuel Bundles by Particle Image Velocimetry", *"XCFD4NRS Experiments and CFD Code Applications to Nuclear Reactor Safety" OECD NEA Workshop,* Grenoble, France, 10-12 September, 2008.

T. Toppila, T.: "Experience with Validation of CFD Methods for Pressure Vessel Downcomer Mixing Analyses", *Technical Meeting on Use of Computational Fluid Dynamics (CFD) Codes for Safety Analysis of Reactor Systems, Including Containment.* Pisa, Italy, 11-14 November (2002).

T. Watanabe, personal communication, February 29, (2008).

S.M. Willemsen, M.J. Komen, "Assessment of RANS CFD modelling for Pressurized Thermal Shock analysis", *The 11th Int. Topical Meeting on Nuclear Reactor Thermal-Hydraulics (NURETH-11)*, Avignon, France, 2-6 October, Paper 121, (2005).